

**"This accepted author manuscript is copyrighted and published by Elsevier. It is posted here by agreement between Elsevier and MTA. The definitive version of the text was subsequently published in [Nuclear Instruments and Methods in Physics Research A 832 (2016) 254–258; DOI 10.1016/j.nima.2016.06.132]. Available under license CC-BY-NC-ND."**

# Coating and functionalization of high density ion track structures by atomic layer deposition

Laura Mättö<sup>1</sup>, Imre M. Szilagyi<sup>2,3,4\*</sup>, Mikko Laitinen<sup>1</sup>, Mikko Ritala<sup>4</sup>, Markku Leskelä<sup>4</sup>, Timo Sajavaara<sup>1</sup>

<sup>1</sup>Department of Physics, University of Jyväskylä, P.O. Box 35 (YFL), FI-40014, Finland

<sup>2</sup>Department of Inorganic and Analytical Chemistry, Budapest University of Technology and Economics, Budapest, Szent Gellért tér 4, H-1111, Hungary

<sup>3</sup>MTA-BME Technical Analytical Research Group, Budapest, Szent Gellért tér 4, H-1111, Hungary

<sup>4</sup>Department of Chemistry, University of Helsinki, Helsinki, P.O. Box 55, FI-00014, Finland

**Email:** imre.szilagyi@mail.bme.hu

## Abstract

In this study flexible TiO<sub>2</sub> coated porous Kapton membranes are presented having electron multiplication properties. 800 nm crossing pores were fabricated into 50 μm thick Kapton membranes using ion track technology and chemical etching. Consecutively, 50 nm TiO<sub>2</sub> films were deposited into the pores of the Kapton membranes by atomic layer deposition using Ti(<sup>i</sup>OPr)<sub>4</sub> and water as precursors at 250 °C. The TiO<sub>2</sub> films and coated membranes were studied by scanning electron microscopy (SEM), X-ray diffraction (XRD) and X-ray reflectometry (XRR). Au metal electrode fabrication onto both sides of the coated foils was achieved by electron beam evaporation. The electron multipliers were obtained by joining

two coated membranes separated by a conductive spacer. The results show that electron multiplication can be achieved using ALD-coated flexible ion track polymer foils.

**Keywords:** nanostructures, oxides, polymers, thin films, coatings, electrical properties

## 1. Introduction

Porous materials with precisely controlled properties, such as pore size and diameter, have several applications in, for instance, filtration [1], gas sensing [2,3], catalysis [4], photocatalysis [5,6], solar cells [7], adsorption [8,9], and biomedical research [10]. Micro-channel plates (MCPs) are special member of these materials, in which a porous membrane is composed of parallelly aligned or crossing tubes. An MCP is an array of miniature electron multipliers that are each acting as a continuous dynode chain. They can be used e.g. in night vision applications, photomultipliers, particle and time-of-flight detectors [11].

One method to fabricate porous films is to shoot single heavy energetic ions through a material to be manipulated. In ion track method [12] these ions with typical energies of several hundred MeVs are generated by means of an accelerator. When these ions hit the target material, they lose their energy by various interactions with the material, and cause excitation and ionization of target electrons (electronic energy loss), projectile excitation and ionization, electron capture, elastic collisions with target atoms (nuclear energy loss) and electromagnetic radiation. For high energy heavy ions the most significant process is the electronic energy loss. The incident ions are chosen in such a way that the energy transfer to the material is large. The electronic energy loss can be well described by the Bethe-Bloch formula and the SRIM software [13]. The incident ion induces ionization and electric

excitation, which in polymers predominantly breaks chemical bonds and a damaged ion track forms.

After the ion irradiation the pore is created via chemical etching process. The shape of the etched pore depends on the etch velocity of the bulk material  $V_b$  (etch rate of undamaged material) and the etch velocity of track line  $V_t$  (etch rate along the track). Both depend on the etching conditions and  $V_t$  is also influenced by the energy loss of the irradiated ions.  $V_t$  increases with increasing energy loss due to higher damage along the ion track [14]. Size of the pore varies with the etching time, as well as the pH and temperature of the solution.

Atomic layer deposition (ALD) is a gas phase thin film deposition method based on surface controlled self-limiting reactions of volatile precursors, which are introduced into the reaction chamber alternately. ALD can be used to coat not only flat substrates, but also complex surfaces and highly porous materials with uniform films having thickness even down to single nanometers [15,16]. These films can be, for instance, insulating oxides or conducting metals, ternary compounds or polymers [17,18]. These features make ALD a convenient choice for modifying the surface properties of various nanostructures [19-21] or even sensitive substrates such as biomaterials [22].

In previous work by others, ion track structures and ALD have been combined to make nanotubes after dissolving the soluble nano templates [23]. On the other hand, ALD has been used to coat with thin films MCP structures made of glass [24], lead glass [25], borosilicate glass [26,27], porous silicon [28] and anodized  $Al_2O_3$  [29]. These ALD-MCP structures showed mostly similar or even better properties than conventional MCPs based on lead glass, and had increased gain and improved stability as a function of extracted charge in several cases. However, all these substrates were rigid materials, and for MCP applications flexible MCP structures might have obvious advantages in several fields (e.g. night vision). Also MCP devices from plastic materials have been previously reported [30,31]. These devices

were made out of porous polymethyl methacrylate (PMMA) having pore size and thickness of 50  $\mu\text{m}$  and 5 mm, respectively. The polymer channels had separate unspecified conductive and emissive low-temperature ALD coatings. The electron yield was amplified with additional conventional MCP stack after the polymer MCP. In ALD coated MCP structures various secondary electron emissive layers were deposited, e.g. MgO, MgO/TiO<sub>2</sub>, TiO<sub>2</sub>, etc [32]. Though TiO<sub>2</sub> is a less common material for secondary electron emission, its easy ALD deposition makes it a good candidate to prepare new MCP structures.

In this study ALD was used to grow TiO<sub>2</sub> films on the sub-micron diameter ion track structures in order to have low-resistivity and enhanced secondary electron production in the pores. The idea was that an <sup>16</sup>O beam releases secondary electrons upon collision with the pore walls. The secondary electron cloud can divide between crossing pores and further increase the number of electrons. With high secondary electron gain, this type of structures could act as low-cost electron multipliers in optical and various detector applications. The substrate for ALD in our case was a highly flexible porous ion track polyimide (Kapton) (Fig. 1).

## **2. Experimental**

Self-supporting 50  $\mu\text{m}$  thick polyimide foils (Kapton from DuPont) were used as substrate material. The foils were irradiated using the JYFL K-130 cyclotron and Radiation Effects Facility (RADEF) irradiation chamber. The used ion was 600 MeV Xe<sup>25+</sup>, the fluence varied from 10<sup>7</sup> to 10<sup>9</sup> ions/cm<sup>2</sup>, and individual irradiations lasted from seconds to thirty minutes. During the irradiations the beam homogeneity and flux were monitored. Irradiation angle was continuously varied between  $\pm 15^\circ$  and the foil was also rotated in order to get crossing ion

tracks in all directions, and thereby minimizing the probability of wide pores due to adjacent tracks.

The irradiated foils were etched in NaOCl solution [33]. The desired pH for the solution was obtained by adding boric acid ( $\text{H}_3\text{BO}_3$ ), and the pH was monitored before and after the etching. The pH was 10.5 in the beginning and 9.9 after the etching had been completed. The etching temperature was  $(60 \pm 2 \text{ }^\circ\text{C})$ , and the etching time was 6 hours. The as-formed pores were imaged using a scanning electron microscope (Hitachi S-4800 FE-SEM), and the pore diameter was measured to be about 800 nm.

In order to both enhance the secondary electron production from the pore surface and make the pore surface resistive, the porous foils were coated by atomic layer deposition with a  $\text{TiO}_2$  layer using TTIP (titanium tetraisopropoxide,  $65 \text{ }^\circ\text{C}$  evaporation temperature) +  $\text{H}_2\text{O}$  as precursors at  $250 \text{ }^\circ\text{C}$ . Each cycle had the following sequence: two times 0.5 s pulse and 1 s purge followed by 0.5 pulse and 15 s purge for TTIP, then the same for  $\text{H}_2\text{O}$ . Ca. 50 nm  $\text{TiO}_2$  was deposited in 1500 cycles in a Picosun Sunale R-150 ALD reactor.

The film thickness (47.7 nm) was determined by X-ray reflectometry (Bruker D8 Advance ) using a  $\text{TiO}_2$  film, which was deposited onto a 100 mm(100) Si wafer under the same conditions as used for the Kapton membranes. The growth rate per cycle corresponds well to the reported value  $0.3 \text{ \AA/cycle}$  [34].

XRD pattern of the reference  $\text{TiO}_2$  film on Si substrate was recorded by a PANalytical X'pert Pro MPD X-ray diffractometer using  $\text{Cu K}_\alpha$  radiation and grazing incidence angle mode.

Consecutively, conducting 20 nm thick Au electrodes were electron beam evaporated on both sides of the ALD coated porous foils in an ultra high vacuum (UHV) environment.

The electron multiplication properties of the prepared foils were studied using a specially made setup (Fig. 2). The primary setup consisted of two coated 50  $\mu\text{m}$  thick polyimide foils which were separated by 2 mm conductive spacer ring. The voltage over the ALD-Kapton

stack was evenly divided using two 1.2 M $\Omega$  resistors. The lower electrode had a fixed potential of  $-1800$  V and the potential of the upper electrode was varied between  $-1625$  V and  $-2000$  V in order to study the electron multiplication. The weak signals from Kapton electron multiplier were amplified by two conventional micro channel plates (MCP). The upper electrode of the MCP was set to a potential of  $-1725$  V.

The operation of the Kapton/TiO<sub>2</sub> multipliers in ion detection was tested by backscattering a 4.8 MeV <sup>16</sup>O<sup>2+</sup> beam from the Pelletron accelerator from a thin Au target towards the foils. The energy of scattered <sup>16</sup>O ions was about 3.6 MeV, and the range in Kapton coated by 50 nm TiO<sub>2</sub> is about 4.1  $\mu$ m as calculated using SRIM. The measurement time for each point was 500 s and the number of events was normalized using the incident ion fluence information obtained from the beam chopper.

### **3. Results and discussion**

The deposition of the ALD TiO<sub>2</sub> film was successful on polyimide even at a growth temperature of 250 °C (Fig. 3). The 50 mm thick Kapton/TiO<sub>2</sub> porous membrane had ca. 800 nm diameter channels penetrating through the whole structure ( $A/R = 62.5$ ). The small cracks visible on the TiO<sub>2</sub> film on surface of the membrane are most likely due to polymer shrinkage during the cooling down after the ALD growth. The thermal expansion coefficient of polyimide is more than ten times higher than the one for TiO<sub>2</sub>. The good quality of coated foils proves the compatibility of ion track technology using polyimide foils with the ALD method even at fairly high deposition temperatures.

To check the conformality of the as-deposited TiO<sub>2</sub> film, the coated membrane was annealed in air using 1 °C/min heating rate up to 600 °C and then keeping the sample at 600 °C for an hour. As a result of the polyimide membrane combustion a porous inorganic membrane was

obtained consisting of aligned TiO<sub>2</sub> nanotubes (Fig. 4a). The wall thickness of the TiO<sub>2</sub> nanotubes was around 50 nm as expected, and it was confirmed that the TiO<sub>2</sub> film covered uniformly the pores all along their length (Fig. 4b). The figure shows that the complete removal of the polymer material joins the nanotubes together. During the annealing of the polymer, the originally cylindrical TiO<sub>2</sub> film in the polymer channels became somewhat distorted, and the planar TiO<sub>2</sub> layers on the top and back side of the membrane were not maintained. Most probably the applied heat and the considerable gas release during the decomposition and combustion of the polymer were responsible for this. In addition, the film thickness of the TiO<sub>2</sub> film was not enough to provide suitable robustness to it as a self-standing structure, which could have withstood the annealing of the polymer.

The structure of the as-deposited reference TiO<sub>2</sub> film was measured by XRD. According to the XRD pattern (not shown here), TiO<sub>2</sub> was present in the anatase form (ICDD 21-1272).

In Fig. 5 the number of pulses recorded from the commercial MCP anode is plotted as a function of the voltage over the ALD-Kapton two foil stack. The two first modes of operation of the device are easily understandable. If the voltage difference over the ALD-Kapton stack is negative, there is no voltage dependence as the possible electrons are accelerated away from the MCP and the count rate of about 12 counts per second is comparable to the background count rate of the MCP, with or without any backscattered oxygen ions. Once the voltage difference over the ALD-Kapton stack turns positive, there is a clear rising trend until the voltage difference of 75 V, which corresponds to electric field of 75 kV/m. Above this the count rate starts to fluctuate and saturate. The obvious explanation for the saturation could be that the maximum count rate for the active area of the ALD-MCP is already reached and higher voltage over the ALD-MCP stack will only increase the pulse height but not the number of pulses. A detailed pulse height analysis study will be performed in the future.



The electron multiplication is not only dependent on the secondary electron production capability of the pore surface material but also on the electron energy. The flight path is longer and therefore also the energy of the electrons is higher for greater pore diameter and it could be that the 800 nm pore diameter these foils had is quite close to the diameter below which electrons do not get enough energy before colliding with the wall to multiply the yield. On the other hand, smaller pore diameter gives better spatial and temporal resolution. One special signal enhancing new property these ion track foils have is due to the crossing of the pores inside the polymer. The electrons can find their way to another pore and generate a strong daughter signal there as well.

#### **4. Conclusions**

In this study we have demonstrated the ability to combine ion track technology and ALD in fabrication of films with electron multiplication properties. 50 nm TiO<sub>2</sub> films were deposited onto 50 μm Kapton foils, which had 800 nm crossing pores prepared previously by ion track method and chemical etching. The results show that electron multiplication can be achieved using the ALD-coated flexible ion track foils, although multiplication is not still strong enough for direct detection, and thus an extra amplification stage is needed, and further studies are required in finding the optimal pore diameter and ALD film thickness.

One additional possibility for applications opens when the supporting organic polymer is etched away like is shown in Fig. 3a, where an array of 800 nm wide TiO<sub>2</sub> nanotubes with 50 nm wall thickness film is prepared after annealing at 600 °C in air. Due to the crossing tracks, the structure is still rigid and could be used as a highly porous substrate in, for instance, cell growth studies or catalysis.

## Acknowledgements

This work was supported under the auspices of Finnish Centre of Excellence Programme (Project No. 213503, 251353 Nuclear and Accelerator Based Physics). I.M.S. thanks for a Marie Curie Intra-European Fellowship (PIEF-GA-2009-235655), an OTKA-PD-109129 grant and a János Bolyai Research Fellowship of the Hungarian Academy of Sciences.

## References

- [1] E.C. Hammel, O.L.R. Ighodaro, O.I. Okoli, *Ceram. Int.* 40 (2014) 1535.
- [2] C. RoyChaudhuri, *Sens. Actuat. B* 210 (2015) 310.
- [3] R.V. Godbole, P. Rao, P.S. Alegaonkar, S. Bhagwat, *Mater. Chem. Phys.* 161 (2015) 135.
- [4] H.J. Jeong, J. W. Kim, D.Y. Jang, J.H. Shim, *J. Power Sources* 291 (2015) 239.
- [5] Kocakusakoglu, M. Daglar, M. Konyar, H.C. Yatmaz, K. Öztürk, *J. Eur. Ceram. Soc.* 35 (2015) 2845.
- [6] O. Czakkel, E. Geissler, I.M. Szilágyi, K. László, *Nanomat. Environ.* 1 (2013) 23.
- [7] Lim, D.Y. Lee, S.A. Patil, N.K. Shrestha, S.H. Kang, Y.C. Nah, W. Lee, S.H. Han, *Mater. Chem. Phys.* 148 (2014) 562.
- [8] S. Gadipelli, Z.X. Guo, *Prog. Mater. Sci.* 69 (2015) 1.
- [9] O. Czakkel, E. Geissler, I.M. Szilágyi, E. Székely, K. László, *J. Coll. Interface Sci.* 337 (2009) 513.
- [10] X. Du, S.Z. Qiao, *Small*, 11 (2015), 392.
- [11] T. Gys, *Nucl. Instr. Meth. A* 787 (2015) 254.
- [12] C. Trautmann, S. Bouffard, R. Spohr, *Nucl. Instr. Meth. B* 116 (1996) 429.

- [13] J. F. Ziegler, J. Biersack, U. Littmark, *The Stopping and Range of Ions in Matter*, Pergamon Press (1985)
- [14] C. Trautmann, W. Brachle, R. Spohr, J. Vetter, N. Angert, *Nucl. Instr. Meth. B* 111 (1996) 70.
- [15] B.J. O'Neill, D.H.K. Jackson, J. Lee, C. Canlas, P.C. Stair, C.L. Marshall, J.W. Elam, T.F. Kuech, J.A. Dumesic, G.W. Huber, *ACS Catal.* 5 (2015) 1804.
- [16] I.M. Szilágyi, E. Santala, M. Heikkilä, V. Pore, M. Kemell, G. Teucher, T. Firkala, E. Färm, T. Nikitin, L. Khriachtchev, M. Räsänen, M. Ritala, M. Leskelä, *Chem. Vapor Dep.* 19 (2013) 149.
- [17] V. Miikkulainen, M. Leskelä, M. Ritala, R.L. Puurunen, *J. Appl. Phys.* 113 (2013) 021301.
- [18] S. M. George, *Chem. Rev.* (110) 2009 111.
- [19] H. Kim, H.B.R. Lee, W.J. Maeng, *Thin Solid Films* 517 (2009) 2563.
- [20] I.M. Szilágyi, D. Nagy, *J. Phys. Conf. Ser.* 559 (2014) 012010.
- [21] C. Detavernier, J. Dendooven, S.P. Sree, K.F. Ludwig, J.A. Martens, *Chem. Soc. Rev.* 40 (2011) 5242.
- [22] I.M. Szilágyi, G. Teucher, E. Härkönen, E. Färm, T. Hatanpää, T. Nikitin, L. Khriachtchev, M. Räsänen, M. Ritala, M. Leskelä, *Nanotechnology* 24 (2013) 245701.
- [23] S.G. Kang, T. Kobayashi, *Mater. Sci. Forum* 449-452 (2004) 1165.
- [24] J. Wang, K. Byrum, M. Demarteau, J. Elam, A. Mane, E. May, R. Wagner, D. Walters, L. Xia, J. Xie, H. Zhao, *Nucl. Instr. Meth. A* 804 (2015) 84.
- [25] D.R. Beaulieu, D. Gorelikov, P. de Rouffignac, K. Saadatmand, K. Stenton, N. Sullivan, A.S. Tremsin, *Nucl. Instr. Meth. A* 607 (2009) 81.

- [26] O.H.W. Siegmund, J.B. McPhate, A.S. Tremsin, S.R. Jelinsky, R. Hemphill, H.J. Frisch, J. Elam, A. Mane, Nucl. Instr. Meth. A 695 (2012) 168.
- [27] J. Xie, K. Byrum, M. Demarteau, E. May, R. Wagner, D. Walters, J. Wang, L. Xia, H. Zhao, Nucl. Instr. Meth. A 824 (2016) 159.
- [28] Franco, Y. Riesen, N. Wyrsh, S. Dunand, F. Powolny, P. Jarron, C. Ballif, Nucl. Instr. Meth. A 695 (2012) 74.
- [29] G. Drobychev, A. Barysevich, K. Delendik, A. Karneyeu, P. Nédélec, D. Sillou, O. Voitik, Nucl. Instr. Meth. A 567 (2006) 290.
- [30] D.R. Beaulieu, D. Gorelikov, H. Klotzsch, P. de Rouffignac, K. Saadatmand, K. Stenton, N. Sullivan, A.S. Tremsin, Nucl. Instr. Meth. A 633 (2011) S59,
- [31] D. Beaulieu, D. Gorelikov, H. Klotzsch, J. Legere, J. Ryan, P. de Rouffignac, K. Saadatmand, K. Stenton, N. Sullivan, A. Tremsin, Nucl. Instr. Meth. A 659 (2011) 394.
- [32] S.J. Jokela , I.V. Veryovkin, A.V. Zinovev, J.W. Elam, A.U. Mane, Q. Peng, Z. Insepov, Phys. Proc. 37 (2012) 740.
- [33] Z. Tian-Cheng, R. Brandt, P. Vater, J. Vetter, Nucl. Tracks Radiat. Measur. 15 (1988) 771.
- [34] M. Ritala, M. Leskelä, L. Niinistö, P. Haussalo, Chem. Mater. 5 (1993) 1174.

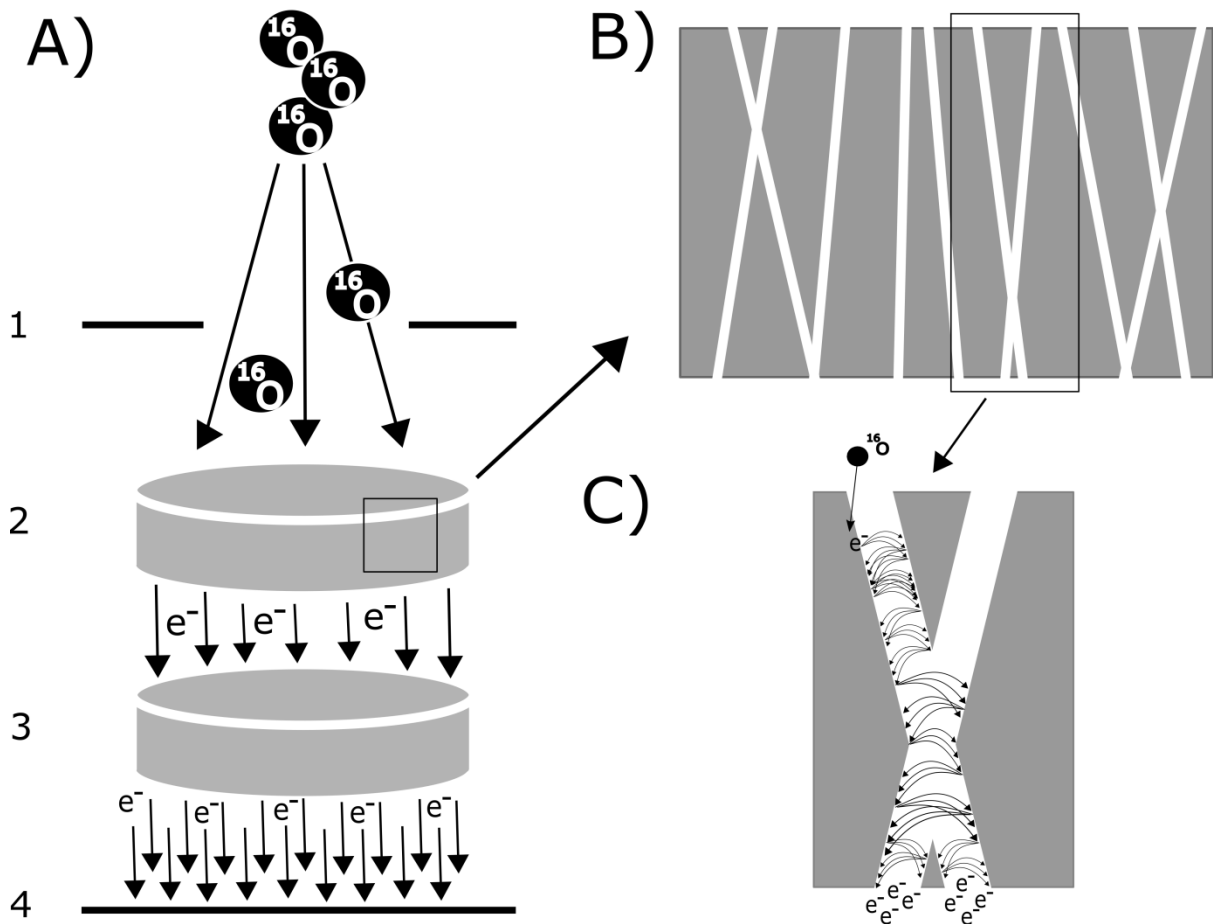


Figure. 1. A) Schematic diagram of the electron multiplier detector configuration. 1) 3,6 MeV  $^{16}\text{O}$  beam and aluminum collimator 2) porous polyimide foil 3) standard MCP used for post amplification of electron signal and 4) charge collecting plate. B) Polyimide foil thickness was  $50\ \mu\text{m}$  and pore diameter  $800\ \text{nm}$ . During the irradiation the foil was tilted between  $0$  and  $15$  degrees. C) The ion beam releases secondary electrons upon collision with the pore walls. The secondary electron cloud can divide between crossing pores and further increase the number of electrons.

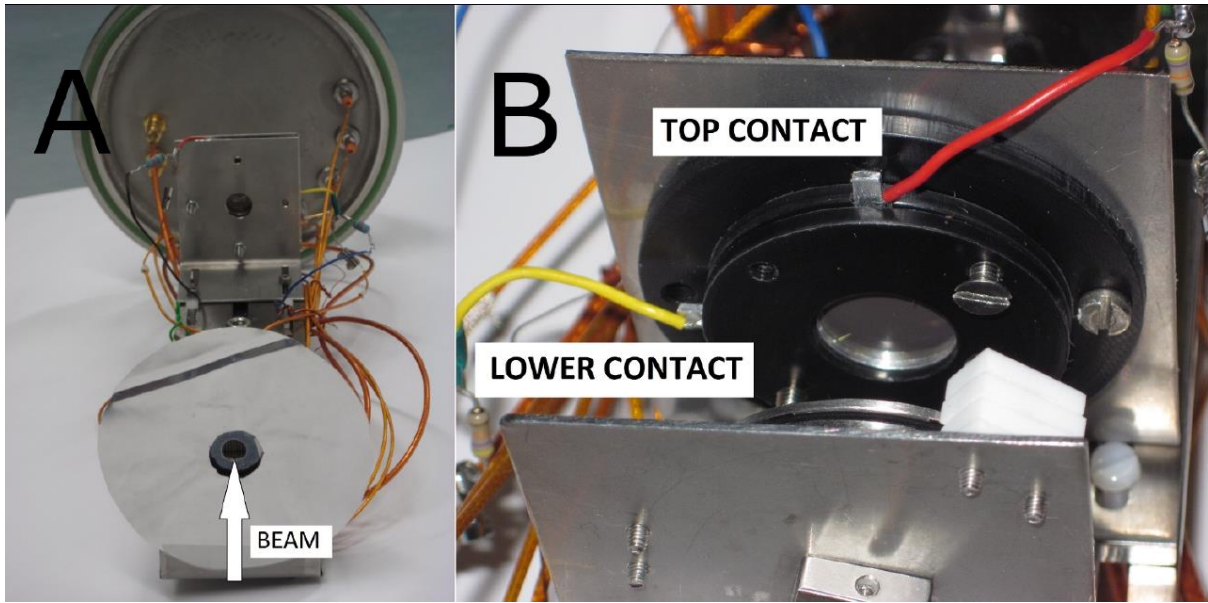


Figure 2. A) A photograph of the used setup showing the collimated entrance to the Kapton/TiO<sub>2</sub> MCP-ALD two foil stack where the scattered 3.6 MeV oxygen beam hits. In B) the same setup is shown from the opposite direction showing the stack and its top and lower contacts as well as the commercial MCP stack which was used to amplify the signal behind the metal plate.

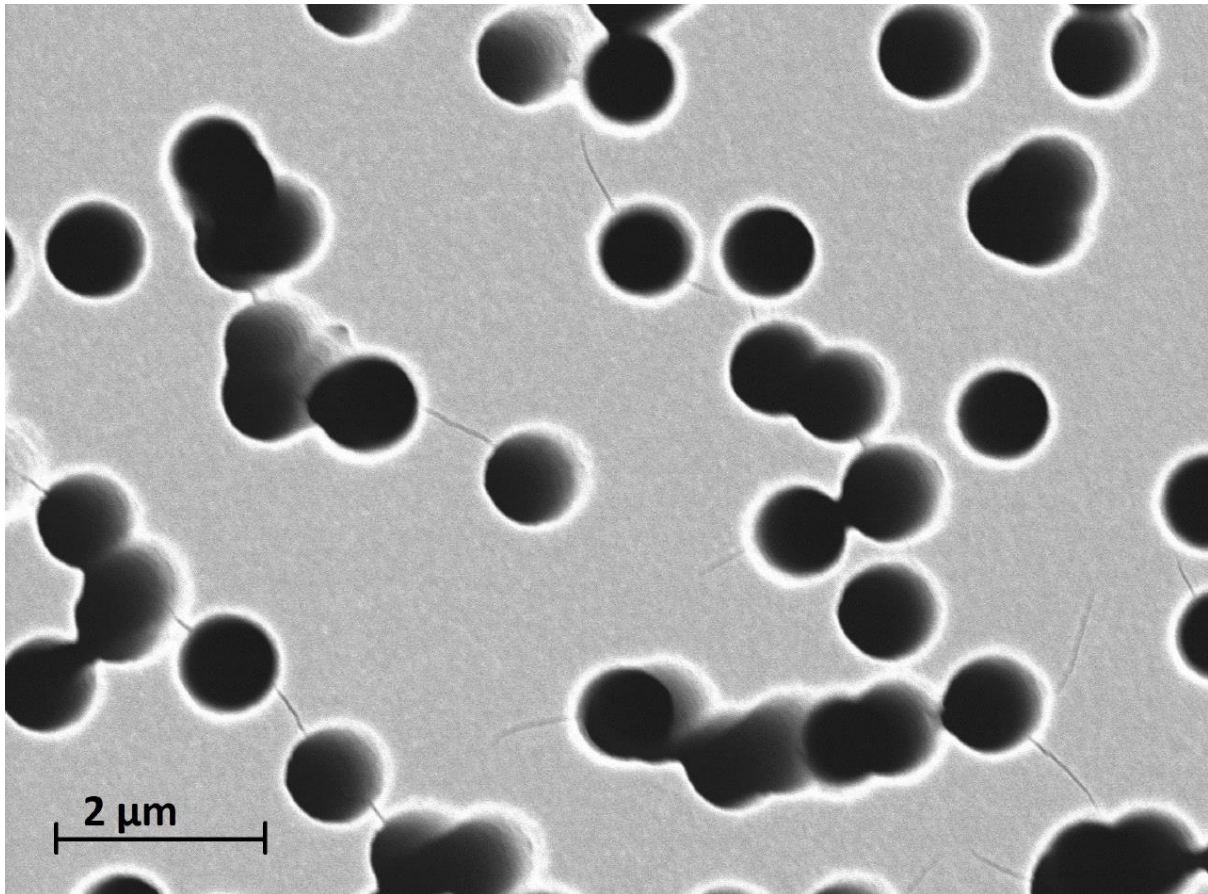


Figure 3. SEM image of the TiO<sub>2</sub> coated porous Kapton membrane. A 50 μm polyimide foil was irradiated with 600 MeV Xe ions and etched for 6 hours in sodium hypochloride and boric acid solutions having pH 10.5. After etching a 50 nm ALD-TiO<sub>2</sub> film was deposited on both sides but also on the pore inner surfaces. The final pore diameter was about 800 nm. The small cracks on the TiO<sub>2</sub> film are most likely due to polymer shrinkage during the cooling down after the ALD growth.

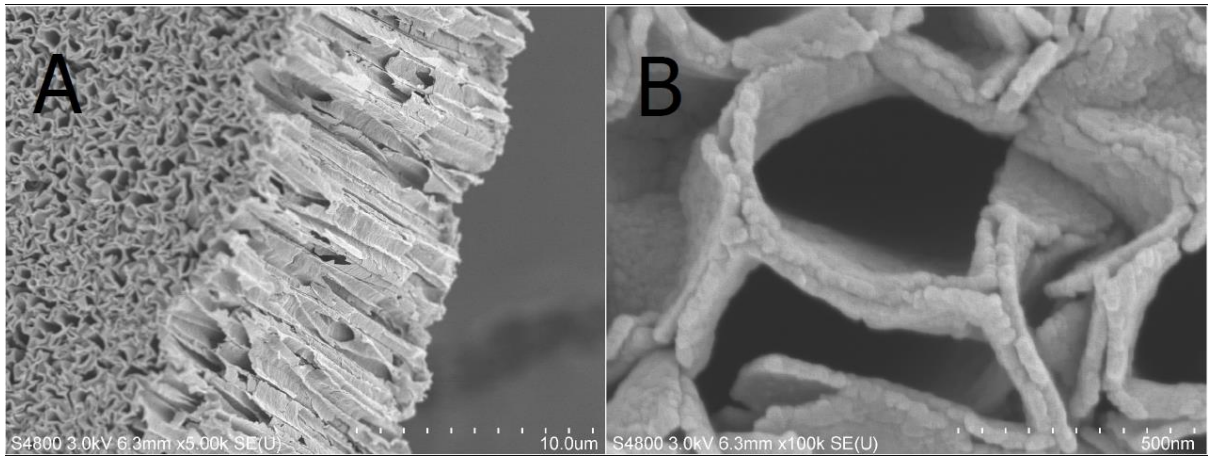


Figure 4. Self-supporting porous ALD  $\text{TiO}_2$  membrane after removal of the polyimide substrate by annealing in air at 600 °C.



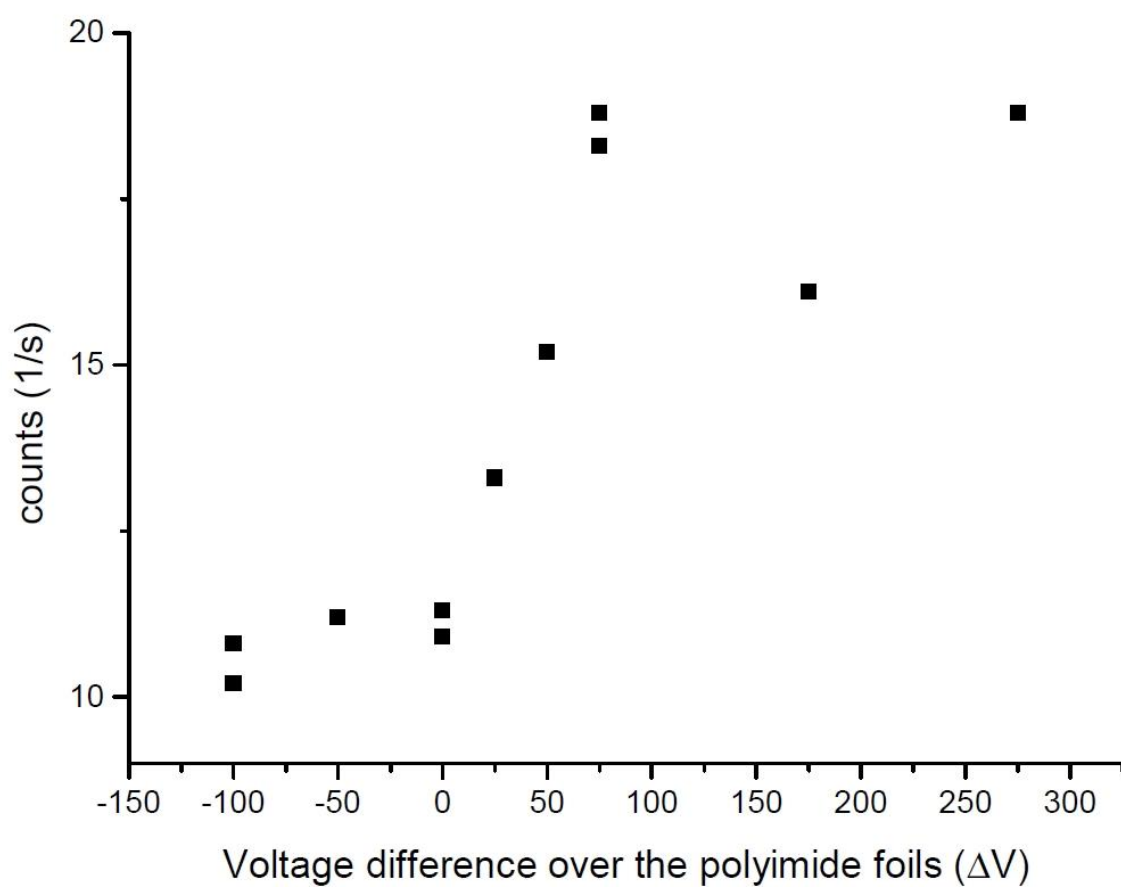


Figure 5. The number of counts per second as a function of the voltage difference over the two foil stack of Kapton/TiO<sub>2</sub> MCP-ALD membranes.